Water Science & Technology

IWA PUBLISHING

Water Science & Technology Vol 87 No 11, 2890 doi: 10.2166/wst.2023.160

Competitive study of homogeneous and heterogeneous Fenton-like flow-through propoxur oxidation in ROC solution

Abed-Alhakeem Azaiza, Raphael Semiat and Hilla Shemer *

Rabin Desalination Laboratory, Department of Chemical Engineering, Technion – Israel Institute of Technology, Haifa 3200003, Israel
*Corresponding author. E-mail: shilla@technion.ac.il

HS, 0000-0001-7588-9690

ABSTRACT

Reverse osmosis is used as a tertiary treatment for wastewater reclamation. However, sustainable management of the concentrate (ROC) is challenging, due to the need for treatment and/or disposal. The objective of this research was to investigate the efficiency of homogeneous and heterogeneous Fenton-like oxidation processes in removing propoxur (PR), a micro-pollutant compound, from synthetic ROC solution in a submerged ceramic membrane reactor operated in a continuous mode. A freshly prepared amorphous heterogeneous catalyst was synthesized and characterized, revealing a layered porous structure of 5–16 nm nanoparticles that formed aggregates (33–49 μm) known as ferrihydrite (Fh). The membrane exhibited a rejection of >99.6% for Fh. The homogeneous catalysis (Fe^{3+}) exhibited better catalytic activity than the Fh in terms of PR removal efficiencies. However, by increasing the H_2O_2 and Fh concentrations at a constant molar ratio, the PR oxidation efficiencies were equal to those catalyzed by the Fe^{3+}. The ionic composition of the ROC solution had an inhibitory effect on the PR oxidation, whereas increased residence time improved it up to 87% at a residence time of 88 min. Overall, the study highlights the potential of heterogeneous Fenton-like processes catalyzed by Fh in a continuous mode of operation.

Key words: ceramic membrane, ferrihydrite, micro-pollutants, reverse osmosis concentrate, submerged membrane reactor

HIGHLIGHTS

- Propoxur removal from ROC solution in a submerged ceramic membrane reactor was studied.
- Homogeneous (Fe^{3+}) and heterogeneous (ferrihydrite) Fenton-like oxidation were compared.
- While Fe^{3+} exhibited better catalytic activity than Fh, increased H_2O_2 and Fh concentrations led to similar PR removal as Fe^{3+}.
- Maximal PR removal of 87% was obtained at a residence time of 88 min.
- The composition of the ROC inhibited the PR oxidation.

1. INTRODUCTION

The ever-increasing application of reverse osmosis (RO) in municipal and industrial wastewater treatment has provided an affordable alternative for the sustainable reclamation of water resources. Nonetheless, this process produces a concentrated waste stream (ROC) that needs to be treated and/or disposed of. Municipal wastewater ROC contains rejected substances at 4–7 times higher concentrations than the feed water (Yaqub *et al.* 2022) and has a reduced volume of 15–20% (Xiang *et al.* 2019). The composition of the ROC depends on the properties of the raw wastewater and the specific wastewater treatment process applied. It consists mainly of nutrients, dissolved inorganic salts, and organic substances such as micro-pollutants (MPs). The range of the physicochemical parameters of ROC can be found in Deng (2020) and Valdés *et al.* (2021).

MPs consist of natural and anthropogenic substances, including pharmaceuticals, personal care products, steroid hormones, industrial chemicals, pesticides, and surfactants. The concentrations of micro-pollutant in ROC range from a few ng/L to hundreds of mg/L. The occurrence of 55 emerging MPs in nanofiltration and RO municipal wastewater concentrates was reviewed by Deng (2020).

Several studies have comprehensively reviewed the physicochemical and biological techniques explored for the removal of MPs, including adsorption, membrane processes, advanced oxidation processes (AOPs), and their integration (Rathi *et al.* 2021; Sivaranjanee & Kumar 2021; Shahid *et al.* 2021; Kumar *et al.* 2022; Morin-Crini *et al.* 2022).

Management of ROC often poses challenges, as removal of organic pollutants from ROC by conventional methods is difficult due to high salinity and the organic pollutants recalcitrant nature. High salinity inhibits microbial activity mainly by causing water loss from the cell membranes and reducing enzyme activities. This can result in plasmolysis or cell death (Shi *et al.* 2015). Additionally, high salinity can impact oxidation processes by scavenging bulk and/or surface oxidants, decreasing dissolution, inactivating active sites, and altering the nature of the organics (Yuan *et al.* 2022).

AOPs are utilized for the partial or complete mineralization of contaminants through *in-situ* generation of highly reactive and low selectivity radicals, including hydroxyl, hydroperoxyl, and superoxide. Sulfate and chloride radicals are also included in a wider definition of AOPs. AOPs are based on ozone, hydrogen peroxide electrochemical reactions, photolysis, sonolysis, and their combinations. Several recent comprehensive reviews have been published on AOPs in general and specifically for treating emerging trace organic contaminants (Giwa *et al.* 2021; Krishnan *et al.* 2021; Tufail *et al.* 2021; Priyadarshini *et al.* 2022; Saravanan *et al.* 2022; Gonzaga *et al.* 2023; Wang *et al.* 2023). Moreover, Xiang *et al.* (2019), Deng (2020), and Arola *et al.* (2019) have reviewed various AOPs that are applicable to ROC treatment for municipal wastewater reclamation.

The Fenton (H_2O_2/Fe^{2+}) and Fenton-like (H_2O_2/Fe^{3+}) reaction can be either homogeneous or heterogeneous, with the latter involving the use of solid catalyst such as iron oxyhydroxide, iron oxides (ferrihydrite, goethite, hematite, and magnetite), and zero-valent iron. Iron-based catalysts have several advantages, including their abundance, low cost, high catalytic activity, low toxicity, efficient recovery, chemically stability over a wide pH environmental friendliness, and sustainability (Hussain *et al.* 2021; Thomas *et al.* 2021). In both Fenton and Fenton-like systems, the primary reactions generate hydroxyl radicals (HO•), hydroperoxy (HO_2•), and peroxide radicals $O_2^{\bullet -}$, as shown in Equations (1)–(3). The rate constant of reaction 1 (40–80 1/M s) is much higher than that of reaction 2 (0.1–1 $\times$ 10^{-2} 1/M s) (Thomas *et al.* 2021), indicating the importance of the Fe^{3+}/Fe^{2+} redox cycle for highly efficient oxidation.

Heterogeneous Fenton-like reactions, catalyzed by iron oxide, are initiated through surface complexation (Equation (4)) followed by a ligand-to-metal electron transfer within the surface complex (Equation (5)). This generates HO_2• and $O_2^{\bullet -}$. Hydroxyl radicals are then formed by the reaction with surface ferrous ions (Equation (6)) (Chen *et al.* 2021). The primary difference in the oxidation mechanism between homogeneous and heterogeneous Fenton processes is that the former occurs in the bulk solution, whereas the latter occurs in the solid–liquid boundary layer and/or on the surface of the heterogeneous catalyst. Leaching of iron from the surface of the heterogeneous catalysts may induce a homogeneous Fenton reaction.

$$Fe^{2+} + H_2O_2 \rightarrow Fe^{3+} + OH^- + OH\cdot \quad (1)$$

$$Fe^{3+} + H_2O_2 \rightarrow Fe^{2+} + H^+ + HO_2\cdot \quad (2)$$

$$OH\cdot + H_2O_2 \rightarrow O_2^-\cdot + H_2O + H^+ \quad (3)$$

$$\equiv Fe^{3+} + H_2O_2 \leftrightarrows \equiv Fe^{3+}(O_2H) + H^+ \quad (4)$$

$$\equiv Fe^{3+}(O_2H) \rightarrow \equiv Fe^{2+} + HO_2\cdot/(O_2^-\cdot + H^+) \quad (5)$$

$$\equiv Fe^{2+} + H_2O_2 \rightarrow \equiv Fe^{3+} + OH^- + OH\cdot \quad (6)$$

The Fenton process is a preferred AOP due to its versatile applications, capacity to withstand interference, simple operation, rapid degradation rate, and improved biodegradability of organic contaminants. However, it exhibits certain limitations such as a restricted operational pH range of 2–4 and the need for neutralization. The formation of iron sludge and consequent discharge of iron into the environment further contribute to its drawbacks (Zhang *et al.* 2019). The heterogeneous Fenton process offers several advantages over the homogeneous Fenton process. These include reduced iron sludge production, a wider working pH range, catalyst reusability, reduced iron leaching, long-term catalyst stability, and effective Fe^{3+}/Fe^{2+} interconversion (Xavier *et al.* 2013; Sreeja & Sosamony 2016; Zhang *et al.* 2019). However, it is limited by the diffusion rate of the target compounds onto the surface of the catalyst and/or its boundary layer, resulting in a slower oxidation rate than the homogeneous process at the same concentrations (Litter & Slodowicz 2017). The catalyst's synthetic conditions and costs, as well as the reactor, pose challangers (Zhang *et al.* 2019).

Propoxur (PR), 2-isopropoxy phenyl *N*-methyl carbamate, commercially known as Baygon® is a broad-spectrum insecticide that can persist in the environment and pose a risk to human health and the ecosystem. It has been detected in surface water, groundwater, and soil, indicating widespread environmental contamination. Exposure to PR has been linked to various adverse health effects, such as nervous system stimulation, enzyme activation, stunted growth, and cancer (Vandana *et al.* 2001). AOPs can be effective for the removal of PR from contaminated water hence contribute to reducing its potential adverse effects on human health and the environment. It has been reported that PR was oxidized via direct photolysis (UV) (Benitez *et al.* 1994; Sanjuán *et al.* 2000), photo-catalysis (UV/TiO_2) (Sanjuán *et al.* 2000), UV/TiO_2/GAC (Lu 1999), O_3/UV (Benitez *et al.* 1994), and electrochemically (Guimarães Selva & Longo Cesar Paixão 2016).

In this study, the removal of PR from synthetic ROC solution by homogeneous and heterogeneous Fenton-like oxidation in a ceramic membrane reactor was compared. PR was chosen as a model MP compound due to its high water solubility and widespread use as a broad-spectrum insecticide.

2. EXPERIMENTAL

2.1. Materials

The chemicals were of analytical grade and were used as-received without further purification. PR was supplied by Supelco (China), NaCl, KCl, $NaHCO_3$ (Frutarom Industries Ltd, Israel), Na_2SO_4 (Bio-Lab Ltd, Israel), $MgCl_2{\cdot}6H_2O$ (Merck, Germany), $CaCl_2{\cdot}2H_2O$ (Spectrum, USA), Na_2HPO_4 (Riedel-de Haën, Germany), and $FeCl_3{\cdot}6H_2O$ (Alfa Aesar, USA).

2.2. Synthetic reverse osmosis concentrate solution

Synthetic ROC solution was prepared by dissolving NaCl, $NaHCO_3$, Na_2SO_4, $CaCl_2{\cdot}2H_2O$, KCl, $Na_2HPO_4{\cdot}2H_2O$, and $MgCl_2{\cdot}6H_2O$ in deionized water (DI). The composition of the solution is listed in Table 1. PR oxidation experiments were conducted in both DI and ROC solutions. It is important to note that the addition of both the homogeneous and heterogeneous catalysts introduces counter ions to the aqueous solution, namely sodium and chloride.

2.3. Synthesis and characterization of the catalyst

A freshly prepared amorphous ferric chloride-based catalyst was synthesized using the precipitation method. The catalyst was prepared by diluting a stock solution of $FeCl_3{\cdot}6H_2O$ (1.3 M) in DI water to the desired concentration, followed by the addition of a predetermined amount of NaOH solution (1.0 M) to achieve the desired pH.

The particle sizes were measured using a laser diffraction particle size analyzer (Mastersizer 2000, Malvern, UK). The zeta potential was measured using a ZetaSizer Nano-ZS analyzer (Malvern, UK) in a disposable folded capillary cell (DTS1060). The morphology of the synthesized catalyst was studied using Philips CM120 Transmission Electron Microscopy (TEM) and an Olympus BH2 Light Microscope connected to an Optronics CCD camera. Raman spectra were obtained with a Horiba Jobin Yvon LABRAM HR micro-Raman spectrometer equipped with a Nd-YAG laser (100 mW, 532.2 nm) and diffraction gratings of 1,800 grooves 1/mm. The Raman shifts were detected using a Peltier-cooled, slow-scan, CCD matrix detector, and ranged from 180 to 450 1/cm.

2.4. Flow-through ceramic membrane reactor

A submerged single silicon carbide ceramic flat sheet membrane (Cerafiltec, Germany) with a pore size of 0.1 μm and filter area of 0.01 m^2 was used in an acrylic glass reactor with dimensions of 14.3 × 3.7 × 2.0 cm (l × w × d). The schematics of the experimental system is shown in Figure 1. A ceramic membrane was chosen since it exhibits a high oxidation resistance, narrow pore size distribution, and high mechanical stability. Mixing was guaranteed by air bubbles generated by an OxyMax 200 air pump (Oase, Germany) at a flow rate of 1.5 L/min. Air-scouring also prevents membrane fouling by the heterogeneous catalyst.

A Masterflex peristaltic pump (model 77800-50, Cole-Parmer, USA) was used to feed a solution containing PR and hydrogen peroxide into the reactor. The flow rates were set at 0.13–0.59 L/h, resulting in residence times (RTs) of 20–90 min. A

Table 1 | Feed synthetic ROC composition (Woo *et al.* 2019)

Ion	Cl^-	HCO_3^-	SO_4^{2-}	Na^+	Ca^{2+}	K^+	PO_4^{3-}	Mg^{2+}	pH	TDS
(mg/L)	1,000	488	250	819	100	70	31	20	7.8	2,778

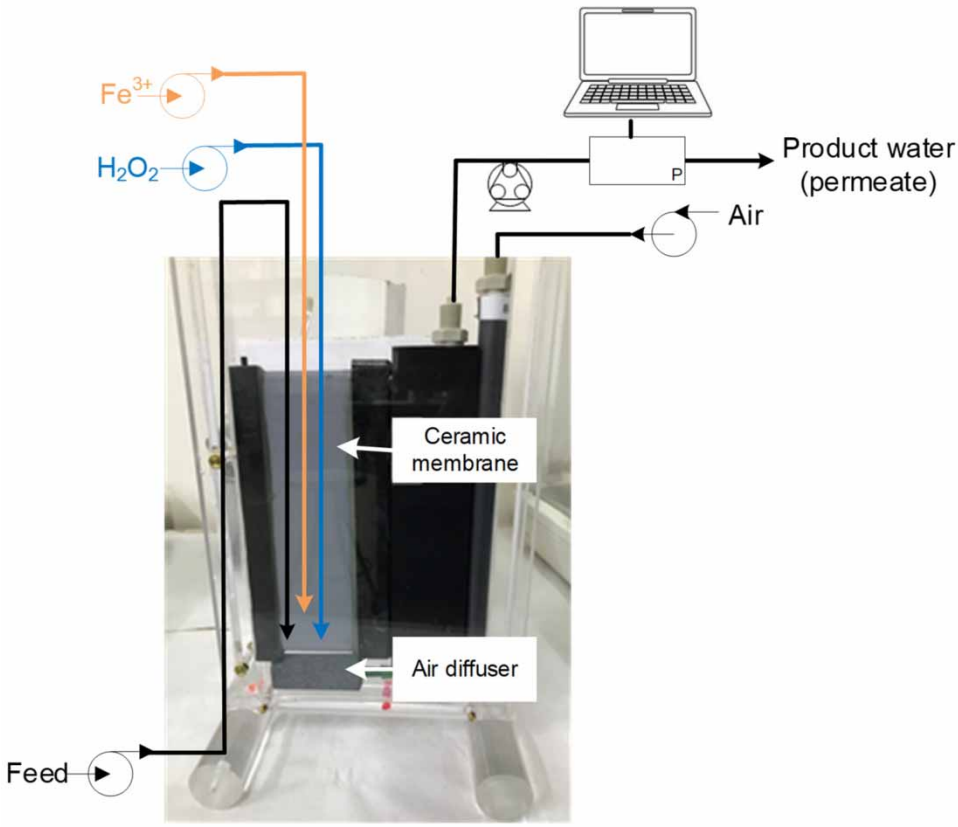

Figure 1 | The submerged ceramic membrane reactor experimental system.

second pump with an identical flow rate was used to pumped the product water (i.e., permeate) at fluxes of 13–59 L/m^2 h and a pressure of <25 mbar. The submerged membrane operated in a dead-end mode.

At the beginning of the experiment, the heterogeneous catalyst was added to the reactor at concentrations ranging from 252 to 1,495 mg/L. The experiments were carried out either in ROC or DI water solutions with a volume of 192 mL, a PR concentration of approximately 1 mg/L, and hydrogen peroxide concentrations ranging from 140 to 1,096 mg/L at molar ratios of 0.7–1.1 iron to hydrogen peroxide. A third pump was used to continuously dose the homogeneous catalyst. These experiments were carried out in ROC solution, at pH 3.0, 150 mg/L H_2O_2, and 250 mg/L Fe^{3+}.

Experiments were conducted to test the effects of sulfate, chloride, and bicarbonate on the PR oxidation in ROC solution, both in the presence and absence of these ions. The experiments were performed at pH 4.0, 150 mg/L H_2O_2, and 250 mg/L catalyst. Notably, these experiments were conducted using a full ROC solution composition, with the omission of one of the aforementioned anions. This is in contrast to the batch to the batch experiments described in the next section, which were carried out in a single salt solution with PR and the tested ion dissolved in DI water.

pH values of 3.0 and 4.0 were maintained constant throughout the experiments using the homogeneous and heterogeneous catalysts, respectively. Experiments were carried out for at least five RTs after the system had reached a steady state. The reported values of C/C_0 represent the normalized concentration at steady-state conditions.

2.5. Batch experiments

The efficiency of batch PR oxidation in ROC solution was investigated using both homogeneous and heterogeneous catalysts. The homogeneous catalyst was tested at pH values of 2.5, 3.0, and 3.5, while the heterogeneous catalyst was tested at pH values of 4.0, 5.0, 6.0, and 7.8. The lowest pH tested for the heterogeneous catalyst was 4, as this is the threshold for ferric chloride coagulation (Wei *et al.* 2017). The pH was maintained constant throughout the experiments. The experiments were conducted in 100 mL glass beakers containing 50 mL of ROC solution with 1 mg/L of PR for up to 4 h. The molar ratio of Fe to H_2O_2 was kept constant at 1, with 84 mg/L of the homogeneous catalyst (50 mg/L H_2O_2) and 250 mg/L of the

heterogeneous catalyst (150 mg/L H_2O_2). The concentrations of the reactants were adjusted to achieve comparable PR removal rates with both catalysts. The solution was stirred using a magnetic stir bar at room temperature (22 ± 2 °C) and sampled periodically to measure the concentrations of PR, hydrogen peroxide, and iron. Prior to analysis, samples were filtered using a 0.45 μm filter to separate the heterogeneous catalysts from the solution.

Batch Fenton-like oxidation experiments designed to study the effect of the catalyst concentration were carried out in a glass beaker containing 25 mL ROC solution with 1 mg/L PR for up to 3.5 h. These experiments were conducted at pH 3.0 and 50 mg/L H_2O_2 for the homogeneous catalyst, and at pH 4.0 and 150 mg/L H_2O_2 for the heterogeneous catalyst. The different reactant concentrations were used so as to obtain similar PR removal efficiencies using both of the catalysts. The catalyst dosages were varied from 8 to 93 mg/L for the homogeneous catalyst and 71 to 256 mg/L for the heterogeneous catalyst, while the oxidant dosage was kept constant.

To examine the effect of accompanying ions on the removal of PR, batch experiments were conducted in the presence of each of the ROC components dissolved in DI water at the concentrations listed in Table 1. The experiments were conducted in glass beakers containing 50 mL of solution for up to 25 min. The homogeneous catalyst was used at pH 3.0 with 25 mg/L H_2O_2, while the heterogeneous catalyst was used at pH 4.0 with 150 mg/L H_2O_2. The molar ratio of Fe to H_2O_2 was kept constant at 1.

The counter ion for the cations (calcium, potassium, and magnesium) was chloride, while the counter ion for the anions (chloride, bicarbonate, phosphate, and sulfate) was sodium. Initially, the effect of the counter ions was tested by dissolving NaCl in DI water at a concentration of 1,628 mg/L. The results served as a benchmark for determining the effect of the other tested ions.

2.6. Analytic methods

The concentration of PR was analyzed using an Agilent 1260 Infinity LC (Agilent, US) equipped with a Zorbax Eclipse XDB-C18 column. The eluent consisted of a 70:30 (v/v) mixture of HPLC-grade acetonitrile and HPLC-grade water, at a flow rate of 0.4 mL/min. PR concentration was measured at a wavelength of 271 nm, using an injection volume of 10 μL, and a column oven temperature of 30 °C.

Hydrogen peroxide concentration was determined by the Ghormley method (Klassen *et al.* 1994). Iron concentration was determined using Hach method 8008 FerroVer® Iron Reagent Powder Pillows (DR2800 spectrophotometer, Hach, Germany). All experiments carried out in triplicate revealed a standard deviation average of up to 8% in PR analysis and 5% in hydrogen peroxide and iron analysis.

3. RESULTS

3.1. Characterization of the heterogeneous catalysts

Amorphous ferric oxi/hydroxide agglomerates were freshly prepared before each experiment through the precipitation method, by the addition of 1 M NaOH to $FeCl_3{\cdot}6H_2O$ solution in DI water at room temperature. TEM images revealed a mesh-like structure of porous aggregated nanoparticles, as shown in Figure 2(a) and 2(b). The aggregates were composed of spherical particles that ranged in size from 5 to 16 nm, as measured by Image-Pro (v10) analysis software. The micrometer mean size of the aggregates ranged from 33 to 44 μm in ROC solution and from 35 to 49 μm in DI water (Figure 2(c)). The structure corresponds to an amorphous Fe(III) hydroxide hydrate known as ferrihydrite (Fh), which is a hydrous iron oxide mineral with a poorly ordered structure composed of small crystallites with a wide range of sizes and shapes, a water content of 15–25% (Cornell *et al.* 1989), and a relatively high specific surface area up to 700 m^2/g (Eusterhues *et al.* 2008).

Smaller aggregates were obtained in the ROC solution as compared to DI water, as seen in Figure 2(c). This is because the electrolyte ions hinder condensation and polymerization processes, resulting in smaller particle sizes (Wei & Semiat 2017). Measurement of the zeta potential (Figure 2(d)) revealed a higher point of zero charge (8.0) in DI water than in ROC solution (6.1). The electrolytes decrease the zeta potential, indicating reduced electrostatic repulsion, initially promoting the aggregation of iron nanoparticles before the ion hindering effect becomes predominant (Wei & Semiat 2017). Also seen in Figure 2(c) is that larger aggregates were obtained in both DI and ROC solutions as the pH was increased. It has been reported that the threshold of ferric chloride coagulation is around pH 4. At pH < 4, repletion between positively charged monomers limits the bridging process. As the pH increases, the generation of polycationic structures is promoted, resulting in precipitated particles in the aqueous solution (Wei *et al.* 2017).

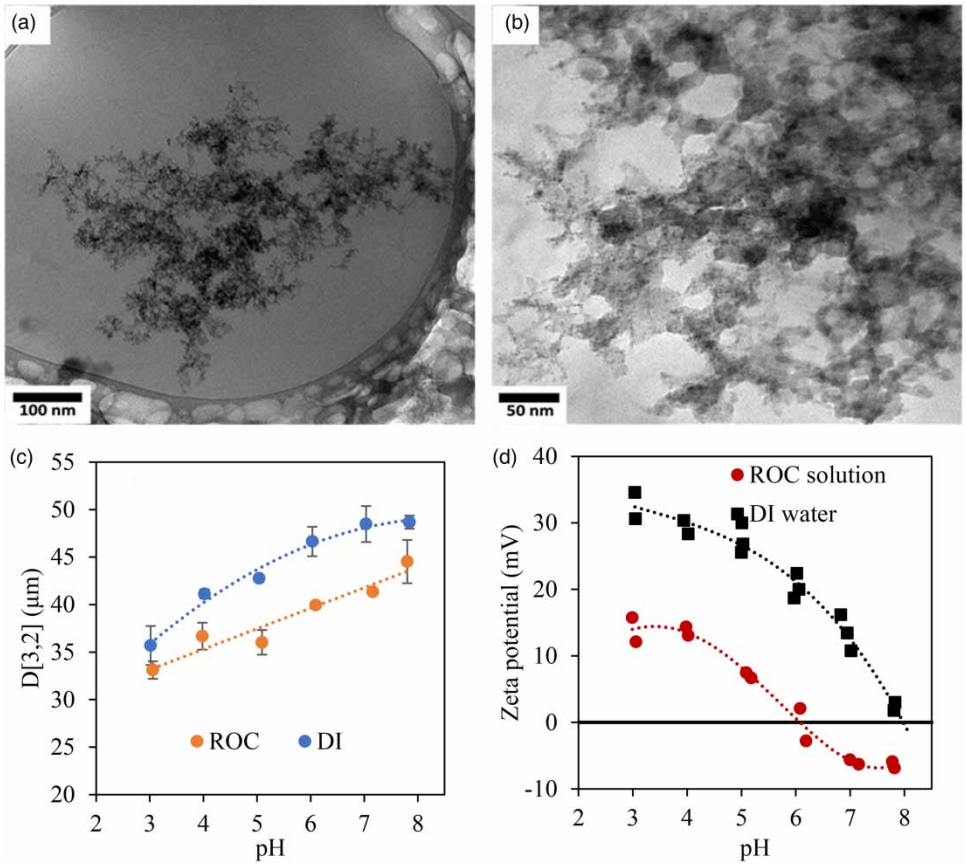

Figure 2 | Aggregates characterization (a and b) Cryo-TEM images, (c) mean aggregate sizes, and (d) zeta potential (4.5 mM Fe).

Air drying of the Fh aggregates (at room temperature) transformed it into hematite, as indicated by the bands of the Raman spectrum in Figure 3. Fe atom vibrations are responsible for the low-frequency modes in the range of 200–300 1/cm, whereas vibrations of O atoms are responsible for bands in the 400–650 1/cm range. The 227 1/cm band is attributed to the movement of iron cations along the *c*-axis. The bands at 410 1/cm are assigned to the symmetric mode of O atoms in relation to other

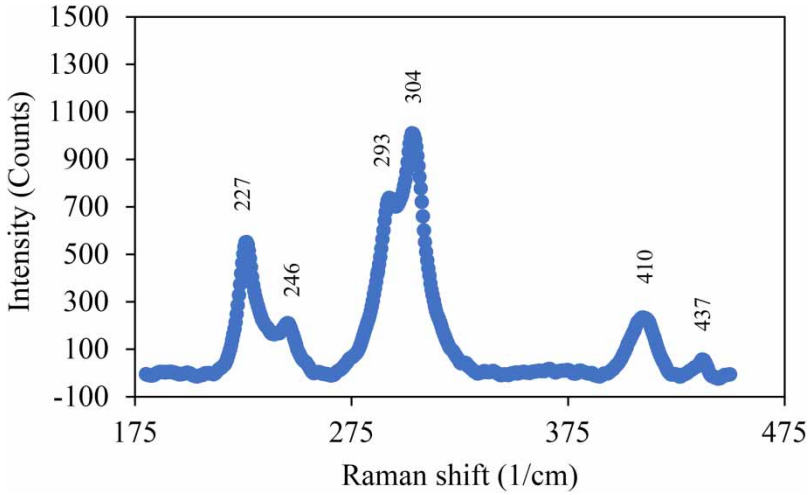

Figure 3 | Raman spectrum of dehydrated Ferrihydrite in room temperature.

cations in a plane that is perpendicular to the crystallographic *c*-axis, and also to Fe–O stretching vibrations (Jain *et al.* 2019). It is reported that Fh is thermodynamically unstable and gradually transforms to either α-FeO(OH) (goethite) by a mechanism of dissolution–precipitation or α-Fe_2O_3 (hematite) by dehydration/internal rearrangement pathway (Hanesch 2009). These crystalline products form by competing mechanisms, and the proportion of each in the final product depends on the relative rates of formation (Cornell *et al.* 1989).

3.2. Fenton-like oxidation of PR

Control experiments were conducted in DI water with PR, PR + H_2O_2 (130 mg/L), and PR + Fh (250 mg/L) at a residence time of 44 min and pH of 4.0. In these experiments, the feed PR concentration was 1 mg/L. The results revealed negligible changes in the PR concentrations, indicating that the ceramic membrane and/or the Fh did not adsorb the PR and the hydrogen peroxide did not oxidize it without a catalyst. An Fh rejection of >99.6% by the ceramic membrane was obtained at pH ≥ 4.0.

Batch experiments were conducted to determine the optimal pH for the PR oxidation using Fe^{3+} and Fh at pH 2.5–3.5 and 4.0–7.8, respectively. Figure 4 displays the PR removal and H_2O_2 decomposition at the tested pH values. The results indicate that pH 3.0 exhibited the highest PR removal catalyzed by the Fe^{3+} (88% within 3 h), while PR was removed at 50 and 57% at pH 2.5 and 3.5, respectively. Corresponding to the PR oxidation, the highest decomposition of hydrogen peroxide was obtained at pH 3.0. Catalysis by Fh exhibited maximal PR removal (95%) at pH 4.0 after 4 h. The removal of PR decreased as the pH increased, with only 16% removed at pH 7.8. Lower hydrogen peroxide decomposition was obtained at an acidic pH.

The pH can have an impact on heterogeneous catalysts by altering the solubility of iron on the catalyst surface and/or activity of its active sites. The fact that the amorphous Fh catalysis was not efficient at elevated pH levels suggests that the pH did not affect its active sites but rather the solubility of iron. An increase in pH slows the iron leaching from the heterogeneous catalyst, leading to inactivation in the bulk solution via hydrolysis and ferric hydroxide sludge precipitation (Wang *et al.* 2016). Homogeneous Fenton reactions are feasible at pH < 4 because the interconversion of Fe^{2+} and Fe^{3+} maximizes the process efficiency (Hussain *et al.* 2021). Acidity aids in protonating hydrogen peroxide, which enhances its reactivity and increases its propensity to produce hydroxyl radicals rather than decomposing into water (Jung *et al.* 2009).

3.2.1. Typical results

Figure 5 displays typical results for the PR and hydrogen peroxide decay during the oxidation reaction by H_2O_2/Fh in the submerged ceramic membrane reactor. The results are presented as a plot of the normalized concentration (C/C_0) as a function of normalized time, i.e., the reaction time divided by the residence time (t/τ). As seen, there are two unique regions in Figure 5. The first region comprises the first 2.3 RTs and is referred to as the start-up of the reactor, where a decay in the PR and hydrogen peroxide concentrations is observed. The second region is from 2.3 RTs onward, at which steady-state conditions prevail. In this region, the experimental points are dispersed around an average value shown in Figure 5 as a solid line.

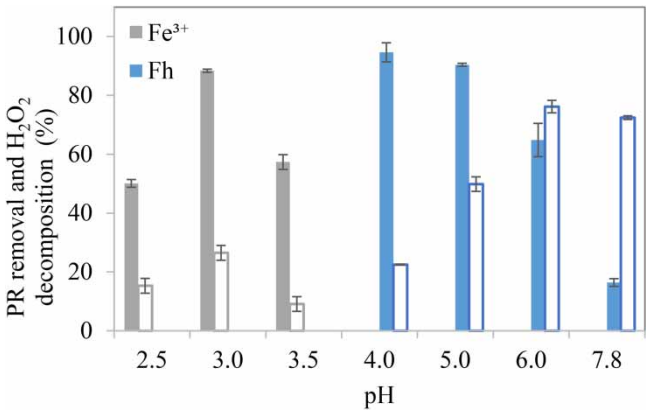

Figure 4 | PR removal (filled columns) and H_2O_2 decomposition (empty columns) as a function of ROC solution pH (Fe^{3+}: 50 mg/L H_2O_2, 84 mg/L Fe^{3+}, $t = 3$ h; Fh: 150 mg/L H_2O_2, 250 mg/L Fh, $t = 4$ h).

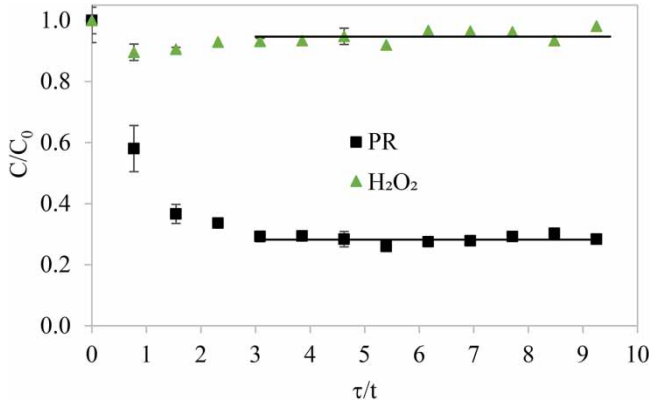

Figure 5 | Propoxur removal and hydrogen peroxide decomposition as a function of the normalized time (DI water, PR = 1 mg/L, H_2O_2 = 150 mg/L, Fh = 260 mg/L, RT of 44 min, pH 4).

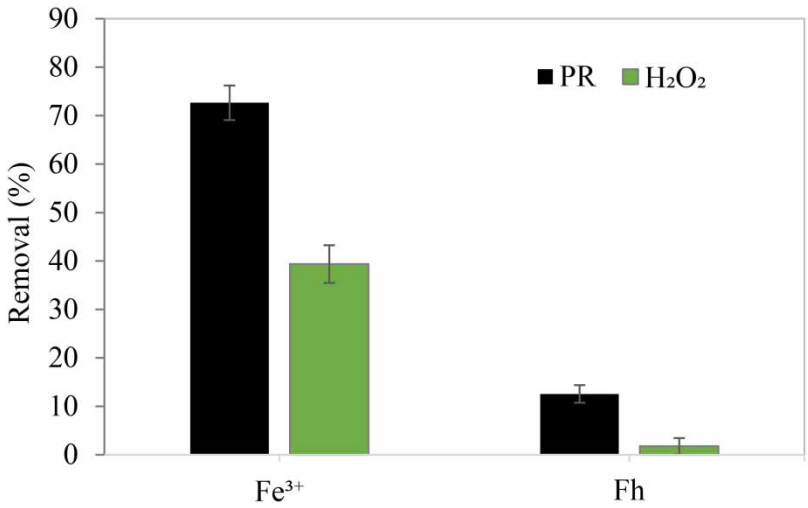

Figure 6 | PR removal and H_2O_2 decomposition catalyzed by Fe^{3+} (pH 3) and Ferrihydrite (pH 4) (ROC solution, PR = 1 mg/L, H_2O_2 = 150 mg/L, Fe = 250 mg/L, RT of 44 min).

3.2.2. Heterogeneous and homogeneous Fenton-like PR oxidation

The removal of PR in ROC solution and hydrogen peroxide decomposition, catalyzed by Fe^{3+} and Fh, were compared. As seen in Figure 6, Fe^{3+} exhibited better catalytic performance than the Fh. In the presence of Fe^{3+}, a total of 72% PR was removed, and 39% of hydrogen peroxide was decomposed, while only 13 and 2%, respectively, were removed in the presence of Fh. A possible explanation for these outcomes could be attributed to the limited mass transfer of the substrates to the heterogeneous catalyst surface (Zhang *et al.* 2013). In addition, the surface area and number of active sites of the catalyst can restrict heterogeneous oxidation (Ioffe *et al.* 2022). Heterogeneous catalysts have low activity due to the slow reduction of Fe^{3+} in the Fe^{3+}/Fe^{2+} redox cycle ($1–3 \times 10^{-3}$ 1/M s) (Gao *et al.* 2020).

3.2.3. Effect of H_2O_2/iron concentration

In order to find the best conditions for the flow-through experiments, the effect of the catalyst concentration on the PR removal was studied in batch experiments. In these experiments, the dosage of catalyst was changed while that of the oxidant was constant. The increase in the catalyst concentration led to an increase in the molar ratio of iron to hydrogen peroxide. As seen in Figure 7, an increase in the molar ratio resulted in augmented removal of the PR, up to a molar ratio of 0.75 with a removal of 93%. A further increase in the molar ratio did not improve the PR removal. It is established that higher catalyst dosages facilitate the Fenton process, particularly when using heterogeneous iron-based catalysts. However, at a certain

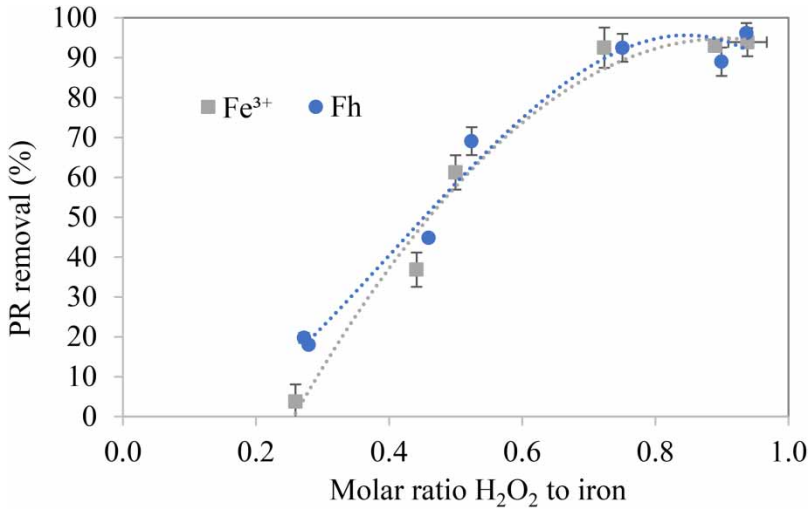

Figure 7 | PR removal as a function of the molar ratio Fe to H_2O_2 using Fe^{3+} (pH 3, $H_2O_2 = 50$ mg/L, $t = 3$ h) and Fh (pH 4, $H_2O_2 = 150$ mg/L, $t = 4$ h) as catalysts (Batch experiments, PR = 1 mg/L).

concentration, the scavenging of hydroxyl radicals by the catalyst itself may inhibit the reaction (Hussain *et al.* 2021). Based on these results, flow-through experiments were conducted using both catalysts, at a molar ratio of 0.75 Fe to H_2O_2.

Both catalysts exhibited similar removal efficiencies at the same molar ratio (Figure 7). However, to achieve equivalent removal percentages as Fe^{3+}, the heterogeneous oxidation required three times higher concentrations of H_2O_2 and Fh, as well as prolonged reaction time. As mentioned earlier, heterogeneous catalysis can be limited by factors such as mass transfer, catalyst surface area, number of active sites, and the reduction rate of Fe^{3+}.

In order to equilibrate the efficiency of PR removal catalyzed by Fh with that of Fe^{3+} in the ceramic membrane reactor, the concentrations of hydrogen peroxide and Fh were increased while keeping the molar ratio of Fe to H_2O_2 constant at 0.75. The reaction was carried out at residence time for 44 min. The results, displayed in Figure 8(a), show a linear relationship between the H_2O_2 and Fh concentrations and PR removal up to 1,100 and 1,500 mg/L H_2O_2 and Fh, respectively. At these concentrations, PR removal (3.6 ± 0.105 μM) was equal to that catalyzed by the Fe^{3+} (3.5 ± 0.157 μM), with higher H_2O_2 decomposition during the heterogeneously catalyzed PR oxidation (Figure 8(b)).

During the homogeneous Fenton-like oxidation process, Fe^{3+} was continuously dosed into the reactor. Initially, about five times as much Fh was added as compared to Fe^{3+} (1,500 and 250 mg/L, respectively). Within about six RTs, the total iron

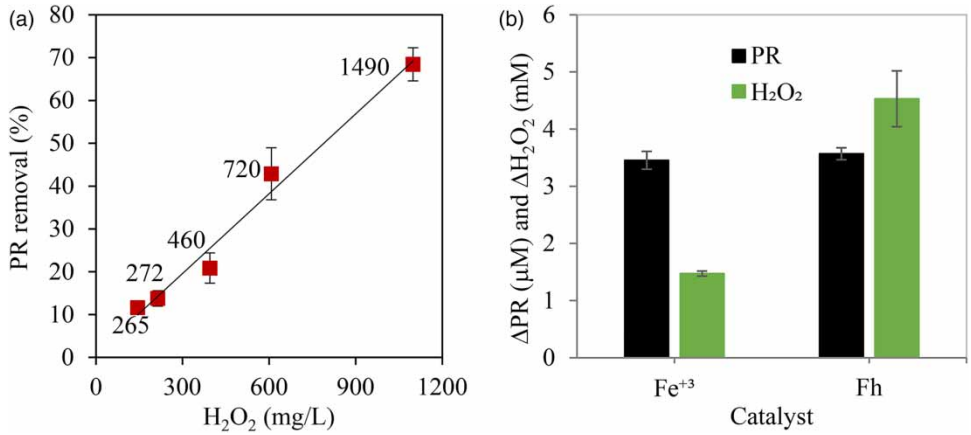

Figure 8 | (a) PR removal at a molar ratio of 0.75 Fe to H_2O_2 as a function of H_2O_2 concentration; data labels are for Fh concentrations; (b) PR removed and H_2O_2 decomposed, catalyzed by Fe^{3+} (pH 3, 150 and 250 mg/L H_2O_2 and Fe^{3+}, respectively) and Fh (pH 4, 1,100 and 1,500 mg/L H_2O_2 and Fh, respectively). ROC solution, PR = 1 mg/L, RT of 44 min.

consumed (253 g/m^3 product water) was equalized for both catalysts, after which the Fe^{3+} concentration exceeded that of the Fh. This suggests a preference for heterogeneous catalysis during prolonged operations, as less Fh would be required. Additionally, using Fh as a catalyst has the added advantage that the product water does not contain any iron.

3.2.4. Effect of residence time

Figure 9 displays the PR removal, catalyzed by Fh, at steady state as a function of residence time (20–90 min) in both DI and ROC solutions. In the ROC solution, the concentrations of the catalyst and oxidants were about 7 times higher (1,500 and 1,100 mg/L, respectively) compared to the DI water solution (250 and 150 mg/L, respectively). This was necessary to achieve higher PR removal efficiencies, as the lower concentrations resulted in only 12 and 30% removal at RTs of 44 and 88 min, respectively. The effect of the ROC ionic composition on the PR oxidation is discussed in detail in the next section.

As seen in Figure 9, a linear relationship was observed in DI water solutions, between residence time and PR removal, with higher removal rates as residence time increased. The highest PR removal of 89.7% was obtained at a RT of 87.5 min. In contrast, an asymptotic relationship between residence time and PR removal was observed in the ROC solution. Only a small change in the PR removal performance was found following the RT of 64 min. Longer RTs typically result in higher removal rates due to increased reaction time. Insufficient contact between the target compounds and the heterogeneous catalyst, as well as the limiting mass transfer rates, may lead to a lower oxidation efficiency (An *et al.* 2022). Nonetheless, PR oxidation catalyzed by Fe^{3+} (150 and 250 mg/L H_2O_2 and Fe^{3+}, respectively) was not affected by the RTs of 20–60 min (data not shown). These results suggest that, for the tested concentrations of the hydrogen peroxide and Fe^{3+}, RT of 20 min was sufficient to effectively remove the PR to a maximum level of 68 $\pm$ 3.4%, and that the reaction rate was shorter than 20 min.

3.2.5. Solution composition

To better understand the effect of the ROC solution on the PR Fenton-like oxidation (both homogenous and heterogeneous), batch experiments were performed in DI water solution with the addition of each of the ROC solution components at the concentrations listed in Table 1. It should be noted that the concentration of the ions may also contribute to their effect on the PR oxidation. The results were compared to those of PR oxidation in NaCl solution (1.6 g/L) in order to eliminate the effect of the counter ions, chloride and sodium, that accompany the tested ions. These experiments were conducted at a molar ratio of 1 Fe to H_2O_2 with six times higher concentrations of H_2O_2 catalyzed by Fh. The higher concentrations were chosen to achieve PR removal within the time frame of Fe^{3+}.

As seen in Figure 10, the cations (i.e., K^+, Ca^{2+}, and Mg^{2+}) exhibited a negligible effect on the PR oxidation. This may be attributed to their inability to scavenge radicals because they are in their maximum oxidation state (Burns *et al.* 1999). The anions, on the other hand, inhibited the PR oxidation in the following decreasing order: $HPO_4^- > HCO_3^- > Cl^-$. While the catalysis by Fe^{3+} was not affected by the sulfate, it had the most inhibitory effect on the PR oxidation catalyzed by Fh. The difference in the inhibitory effect of the sulfate in the presence of Fe^{3+} and Fh may be attributed to the different pH values at which the oxidation took place (3 and 4, respectively). Sulfate forms a complex with ferric ions at pH >3.5, resulting in the precipitation of $Fe_2(SO_4)_3$ (Barik & Mohapatra 2011); thus, it only affected the Fh catalysis.

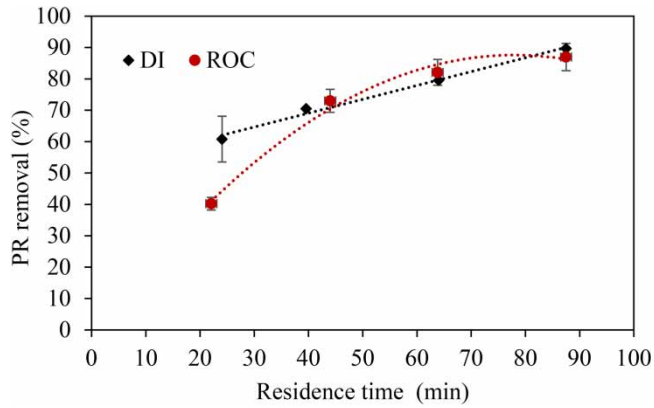

Figure 9 | PR removal in DI water and ROC solutions as a function of residence times at pH 4 (PR = 1 mg/L, DI water solution: H_2O_2 = 150 mg/L, Fh = 260 mg/L; ROC solution: H_2O_2 = 1,000 mg/L, Fh = 1,470 mg/L).

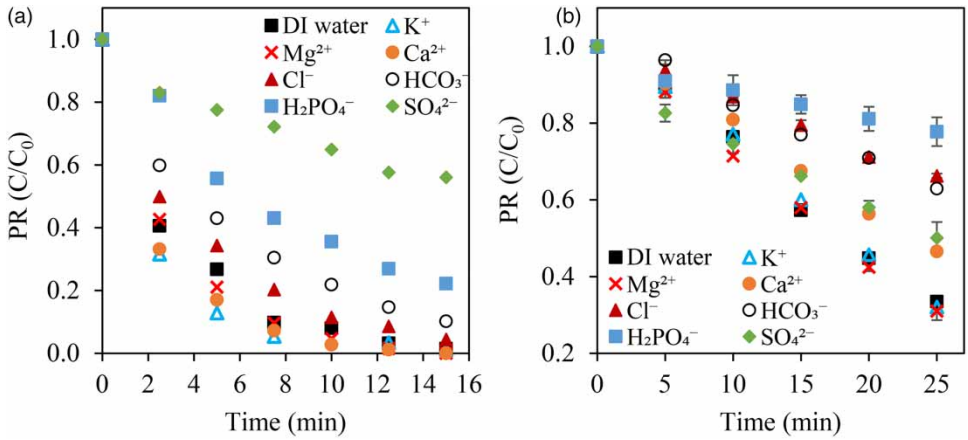

Figure 10 | Propoxur decay in the presence of each of the ROC components during oxidation at a molar ratio of 1 Fe to H_2O_2 (a) Fh catalysis ($H_2O_2 = 150$ mg/L, pH 4.0) and (b) Fe^{3+} catalysis ($H_2O_2 = 25$ mg/L, pH 3.0).

Inorganic ions may inhibit AOPs through two main mechanisms: hydroxyl radical scavenging and iron complexation. Table 2 lists the reactions of the inorganic anions present in the ROC solution with hydroxyl radicals. These inorganic radicals exhibit lower reactivity, higher selectivity, and longer half-lives than hydroxyl radicals (De Laat *et al.* 2004; Patra *et al.* 2020). Inorganic anions may also interfere with the formation of $O_2{\cdot}^-/HO_2{\cdot}$ radicals hindering the regeneration of Fe^{2+} from Fe^{3+} reduction (Equation (2)), resulting in lower hydroxyl radicals generation (Equations (1); De Laat *et al.* 2004).

The complexation of anions with aqueous and/or surface-bound Fe^{2+} and Fe^{3+} affects the distribution and reactivity of the iron species (De Laat *et al.* 2004) for both homogeneous and heterogeneous catalysts. For heterogeneous catalysis, surface complexations may block active sites on the Fh surface, decreasing the oxidation efficiency (Sheng *et al.* 2020). The four anions' surface complexation on Fh is considered inner-sphere for phosphate and carbonate, outer-sphere for chloride, and both inner- and outer-sphere for sulfate, depending on the pH, ionic strength, surface coverage, and hydration (Kumar *et al.* 2014). The molecular structure of sulfate inner-sphere complexes was determined as bidentate – binuclear (Gu *et al.* 2016) while that of carbonate and phosphate double-corner bidentate complexes (Kumar *et al.* 2014). In the solution, sulfate, chloride, and phosphate anions form complexes such as $FeSO_4^+$, $FeSO_4$, $FeCl^{2+}$, $FeCl^+$ (de Oliveira *et al.* 2015), $FeH_2PO_4^{2+}$, $FeHPO_4^+$, and $Fe(H_2PO_4)_2^+$ (Al-Sogair *et al.* 2002).

To further explore the impact of $SO_4{}^{-2}$, HCO_3^-, and Cl^- on PR oxidation, flow-through experiments were conducted in the absence of these anions. It is important to note that unlike the batch experiments, which were conducted in a single salt solution, the experiments described here were carried out in the full ROC composition, with one of the above-mentioned anions excluded. These anions were selected due to their significant effect on Fh-catalyzed PR oxidation, with Cl^- having the highest concentration in the ROC solution. As expected, excluding the anions from the ROC solution did not significantly affect the oxidation of the PR under steady-state conditions (Figure 11(a)). The number of active sites available for continuous catalytic cycles is one order of magnitude lower than the total anions fed to the reactor: 0.57 mmol sites and 5.88–7.88 mmol of total

Table 2 | Primary reactions of hydroxyl radical with inorganic anions

Reaction	Rate constant (1/M s)	Ref.
$Cl^- + {\cdot}OH \rightarrow ClOH^{-\cdot}$	4.3×10^9	Buxton *et al.* (1998)
$HSO_4^- + {\cdot}OH \rightarrow SO_4^- \cdot + H_2O$	1.4×10^7	de Oliveira *et al.* (2015)
$SO_4^{2-} + {\cdot}OH + H^+ \rightarrow SO_4^- \cdot + H_2$		Kim *et al.* (2019)
$HCO_3^- + {\cdot}OH \rightarrow CO_3^- \cdot + H_2O$	8.5×10^6	Buxton *et al.* (1998)
$CO_3^{2-} + {\cdot}OH \rightarrow CO_3^- \cdot + OH^-$	3.9×10^8	Buxton *et al.* (1998)
$H_2PO_4^- + {\cdot}OH \rightarrow H_2PO_4^- \cdot / HPO_4^- \cdot + OH^- / H_2O$	2.2×10^6	Martire & Gonzalez (2001)
$HPO_4^{2-} + {\cdot}OH \rightarrow HPO_4^- \cdot / PO_4^{2-} \cdot + OH^- / H_2O$	8.0×10^5	Martire & Gonzalez (2001)
$H_3PO_4 + {\cdot}OH \rightarrow H_2PO_4 \cdot + H_2O$	2.6×10^6	Martire & Gonzalez (2001)

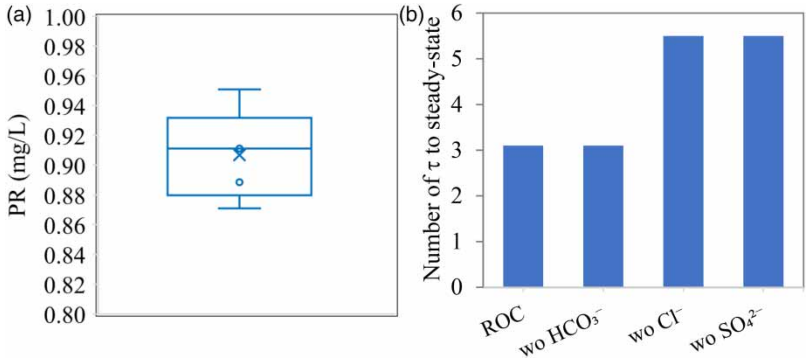

Figure 11 | (a) Box-whisker plot of the PR steady-state concentrations and (b) number of residence times required to reach steady state in full ROC composition and ROC excluding HCO_3^-, SO_4^{2-}, and Cl^- (PR = 1 mg/L, H_2O_2 = 150 mg/L, Fh = 250 mg/L, RT of 44 min, pH 4).

anions, based on a two-line Fh site density of 0.112 mol sites/mol Fe (Chen *et al.* 2021). This indicates that there is an excess of anions competing for the available surface sites for complexation, even when one of the anions is excluded. The binding of the anions to the Fh surface sites hinders surface reactions by decreasing the number of surface sites available for reaction with H_2O_2 and PR. The absence of sulfate and chloride affected the number of RTs required to reach steady state, as illustrated in Figure 11(b). These results may suggest that outer-sphere complexation is the predominant mechanism of the anion adsorption onto the Fh in the ROC solution, as bicarbonate, which forms only inner-sphere complexation, has a negligible effect on the number of RTs required to reach steady state.

4. CONCLUDING REMARKS

The removal of PR from synthetic ROC solution was studied using homogeneous (Fe^{3+}) and heterogeneous (Fh) Fenton-like oxidation in a submerged ceramic membrane reactor was studied. The freshly synthesized heterogeneous Fh catalyst had an amorphous, layered, porous structure consisting of nanoparticles (5–16 nm) in aggregates with a pH_{PZC} of 6.1. The size of the aggregates ranged from 33 to 49 μm, depending on the pH of the solution.

Batch experiments revealed that the most favorable conditions for PR oxidation were achieved at a molar ratio of 0.75 iron to hydrogen peroxide and pH values of 3.0 and 4.0 for homogeneous and heterogeneous catalysis, respectively. The flow-through experiments showed that Fe^{3+} exhibited higher catalytic activity than Fh, with 72 and 13% of PR removed and 39 and 2% of hydrogen peroxide consumed, respectively. By increasing the concentrations of hydrogen peroxide and Fh, the PR removal could be increased to comparable levels as those obtained by Fe^{3+} catalysis. Although Fh required about five times higher reactant concentrations, the total iron consumed was equal to that of the Fe^{3+} within six RTs. After which, the Fe^{3+} concentration exceeded that of the Fh, as ≥99.6% rejection of the Fh was obtained by the ceramic membrane. Hence, for prolonged operations, less Fh would be required. A maximal PR removal of 87% was obtained at a residence time of 88 min.

The ionic composition of the ROC solution was found to inhibit the PR oxidation, requiring higher reactant concentrations to achieve the same removal efficiencies as in DI water solution. PR oxidation in a single salt solution of the ROC composition revealed a negligible effect of the cations, while, the anions hindered PR removal by scavenging hydroxyl radicals and forming iron complexations. Under steady-state conditions, excluding bicarbonate, sulfate, or chloride from the ROC solution did not significantly affect PR oxidation. However, in the absence of sulfate and chloride, the number of RTs required to reach steady state increased, suggesting that outer-sphere complexation is the predominant mechanism of the anion adsorption onto the Fh in the ROC solution.

ACKNOWLEDGEMENTS

The authors would like to express their gratitude for the funding provided by the German Ministry of Education and Research (BMBF) and Israeli Ministry of Science & Technology (MOST) through the German-Israeli water technology cooperation (project WT1902).

DATA AVAILABILITY STATEMENT

All relevant data are included in the paper or its Supplementary Information.

CONFLICT OF INTEREST

The authors declare there is no conflict.

REFERENCES

Al-Sogair, F., Marafie, H. M., Shuaib, N. M., Youngo, H. B. & El-Ezaby, M. S. 2002 Interaction of phosphate with iron(III) in acidic medium, equilibrium and kinetic studies. *Journal of Coordination Chemistry* **55**, 1097–1109.

An, Z., Hu, Y., Zhang, D., Zhou, H., Zhan, J. & Wu, M. 2022 Preparation of MoS_2/SiO_2 composites as fixed-bed reactors for Fenton-like advanced oxidation of sulfonamides in water. *Journal of Environmental Chemical Engineering* **10** (3), 107867.

Arola, K., Van der Bruggen, B., Mänttäri, M. & Kallioinen, M. 2019 Treatment options for nanofiltration and reverse osmosis concentrates from municipal wastewater treatment: a review. *Critical Reviews in Environmental Science and Technology* **49** (22), 2049–2116.

Barik, R. & Mohapatra, M. 2011 Facile precipitation and phase formation of iron oxide with in situ Fe(II) in $Fe_2(SO_4)_3$-NaOH-(N_2H_4) $2H_2SO_4$-H_2O medium. *Indian Journal of Chemical Technology* **18**, 107–112.

Benitez, F. J., Beltran-Heredia, J. & Gonzalez, T. 1994 Kinetic study of propoxur oxidation by UV radiation and combined O_3/UV radiation. *Industrial & Engineering Chemistry Research* **33** (5), 1264–1270.

Burns, R. A., Crittenden, J. C., Hand, D. W., Selzer, V. H., Sutter, L. L. & Salman, S. R. 1999 Effect of inorganic ions in heterogenous photocatalysis of TCE. *Journal of Environmental Engineering* **125** (1), 77–85.

Buxton, G. V., Greenstock, C. L., Helman, W. P. & Ross, A. B. 1998 Critical review of rate constants for reactions of hydrated electrons, hydrogen atoms and hydroxyl radicals ($\cdot OH/\cdot O^-$) in aqueous solution. *Journal of Physical and Chemical Reference Data* **17** (2), 513–886.

Chen, Y., Miller, C. J. & Waite, T. D. 2021 Heterogeneous Fenton chemistry revisited: mechanistic insights from ferrihydrite-mediated oxidation of formate and oxalate. *Environmental Science & Technology* **55**, 14414–14425.

Cornell, R. M., Giovanoli, R. & Schneider, W. 1989 Review of the hydrolysis of iron(III) and the crystallization of amorphous iron(III) hydroxide hydrate. *Journal of Chemical Technology & Biotechnology* **46**, 115–134.

De Laat, J., Le, T. G. & Legube, B. 2004 A comparative study of the effects of chloride, sulfate and nitrate ions on the rates of decomposition of H_2O_2 and organic compounds by Fe(II)/H_2O_2 and Fe(III)/H_2O_2. *Chemosphere* **55**, 715–723.

Deng, H. 2020 A review on the application of ozonation to NF/RO concentrate for municipal wastewater reclamation. *Journal of Hazardous Materials* **391**, 122071.

de Oliveira, T. D., Martini, W. S., Santos, M. D. R., Matos, M. A. C. & da Rocha, L. L. 2015 Caffeine oxidation in water by Fenton and Fenton-like processes: effects of inorganic anions and ecotoxicological evaluation on aquatic organisms. *Journal of the Brazilian Chemical Society* **26**, 178–184.

Eusterhues, K., Wagner, F. E., Häusler, W., Hanzlik, M., Knicker, H., Totsche, K. U., Kögel-Knabner, I. & Schwertmann, U. 2008 Characterization of Ferrihydrite-soil organic matter coprecipitates by X-ray diffraction and Mossbauer. *Environmental Science & Technology* **42**, 7891–7897.

Gao, C., Su, Y., Quan, X., Sharma, V. K., Chen, S., Yu, H., Zhang, Y. & Niu, J. 2020 Electronic modulation of iron-bearing heterogeneous catalysts to accelerate Fe(III)/Fe(II) redox cycle for highly efficient Fenton-like catalysis. *Applied Catalysis B: Environmental* **276**, 119016.

Giwa, A., Yusuf, A., Balogun, H. A., Sambudi, N. S., Bilad, M. R., Adeyemi, I., Chakraborty, S. & Curcio, S. 2021 Recent advances in advanced oxidation processes for removal of contaminants from water: a comprehensive review. *Process Safety and Environmental Protection* **146**, 220–256.

Gonzaga, I. M. D., Almeida, C. V. S. & Mascaro, L. H. 2023 A critical review of photo-based advanced oxidation processes to pharmaceutical degradation. *Catalysts* **13**, 221.

Gu, C., Wang, Z., Kubicki, J. D., Wang, X. & Zhu, M. 2016 X-ray absorption spectroscopic quantification and speciation modeling of sulfate adsorption on Ferrihydrite surfaces. *Environmental Science and Technology* **50** (15), 8067–8076.

Guimarães Selva, T. M. & Longo Cesar Paixão, T. R. 2016 Electrochemical quantification of propoxur using a boron-doped diamond electrode. *Diamond and Related Materials* **66**, 113–118.

Hanesch, M. 2009 Raman spectroscopy of iron oxides and (oxy)hydroxides at low laser power and possible applications in environmental magnetic studies. *Geophysical Journal International* **177**, 941–948.

Hussain, S., Aneggi, E. & Goi, D. 2021 Catalytic activity of metals in heterogeneous Fenton-like oxidation of wastewater contaminants: a review. *Environmental Chemistry Letters* **19**, 2405–2424.

Ioffe, M., Kundu, S., Perez-Lapid, M. & Radian, A. 2022 Heterogeneous Fenton catalyst based on clay decorated with nano-sized amorphous iron oxides prevents oxidant scavenging through surface complexation. *Chemical Engineering Journal* **433**, 134609.

Jain, S., Shah, J., Negi, N. S., Sharma, C. & Kotnala, R. K. 2019 Significance of interface barrier at electrode of hematite hydroelectric cell for generating ecopower by water splitting. *International Journal of Energy Research* **43** (9), 1–13.

Jung, Y. S., Lim, W. T., Park, J. Y. & Kim, Y. H. 2009 Effect of pH on Fenton and Fenton-like oxidation. *Environmental Technology* **30**, 183–190.

Kim, J., Choe, Y. J., Kim, S. H. & Jeong, K. 2019 Enhancing the decomposition of refractory contaminants on SO_4^{2-} functionalized iron oxide to accommodate surface $SO_4^{\cdot-}$ generated via radical transfer from $^{\cdot}OH$. *Applied Catalysis B: Environmental* **252**, 62–76.

Klassen, N. V., Marchington, D. & McGowan, H. C. E. 1994 H_2O_2 determination by the I_3^- method and by $KMnO_4$ titration. *Analytical Chemistry* **66** (18), 2921–2925.

Krishnan, R. Y., Manikandan, S., Subbaiya, R., Biruntha, M., Govarthanan, M. & Karmegam, N. 2021 Removal of emerging micropollutants originating from pharmaceuticals and personal care products (PPCPs) in water and wastewater by advanced oxidation processes: a review. *Environmental Technology & Innovation* **23**, 101757.

Kumar, E., Bhatnagar, A., Hogland, W., Marques, M. & Sillanpää, M. 2014 Interaction of inorganic anions with iron-mineral adsorbents in aqueous media – a review. *Advances in Colloid and Interface Science* **203**, 11–21.

Kumar, R., Qureshi, M., Vishwakarma, D. K., Al-Ansari, N., Kuriqi, A., Elbeltagi, A. & Saraswat, A. 2022 A review on emerging water contaminants and the application of sustainable removal technologies. *Case Studies in Chemical and Environmental Engineering* **6**, 100219.

Litter, M. I. & Slodowicz, M. 2017 An overview on heterogeneous Fenton and photoFenton reactions using zerovalent iron materials. *Journal of Advanced Oxidation Technologies* **20** (1), 20160164.

Lu, M. C. 1999 Photocatalytic oxidation of propoxur insecticide with titanium dioxide supported on activated carbon. *Journal of Environmental Science & Health Part B* **34** (2), 207–223.

Martire, D. O. & Gonzalez, M. C. 2001 Aqueous phase kinetic studies involving intermediates of environmental interest: phosphate radicals and their reactions with substituted benzenes. *Progress in Reaction Kinetics and Mechanism* **26**, 201–218.

Morin-Crini, N., Lichtfouse, E., Fourmentin, M., Ribeiro, A. R. L., Noutsopoulos, C., Mapelli, F., Fenyvesi, E., Vieira, M. G. A., Picos-Corrales, L. A., Moreno-Pirajan, J. C., Giraldo, L., Sohajda, T., Huq, M. M., Soltan, J., Torri, G., Magureanu, M., Bradu, C. & Crini, G. 2022 Removal of emerging contaminants from wastewater using advanced treatments: a review. *Environmental Chemistry Letters* **20**, 1333–1375.

Patra, S. G., Mizrahi, A. & Meyerstein, D. 2020 The role of carbonate in catalytic oxidations. *Accounts of Chemical Research* **53** (10), 2189–2200.

Priyadarshini, M., Das, I., Ghangrekar, M. M. & Blaney, L. 2022 Advanced oxidation processes: performance, advantages, and scale-up of emerging technologies. *Journal of Environmental Management* **316**, 115295.

Rathi, S. B., Kumar, S. P. & Show, P.-L. 2021 A review on effective removal of emerging contaminants from aquatic systems: current trends and scope for further research. *Journal of Hazardous Materials* **409**, 124413.

Sanjuán, A., Aguirre, G., Álvaro, M., García, H. & Scaiano, J. C. 2000 Degradation of propoxur in water using 2,4,6-triphenylpyrylium–Zeolite Y as photocatalyst: product study and laser flash photolysis. *Applied Catalysis B: Environmental* **25** (4), 257–265.

Saravanan, A., Deivayanai, V. C., Kumar, P. S., Rangasamy, G., Hemavathy, R. V., Harshana, T., Gayathri, N. & Alagumalai, K. 2022 A detailed review on advanced oxidation process in treatment of wastewater: mechanism, challenges, and future outlook. *Chemosphere* **308** (3), 136524.

Shahid, M. K., Kashif, A., Fuwad, A. & Choi, Y. 2021 Current advances in treatment technologies for removal of emerging contaminants from water – a critical review. *Coordination Chemistry Reviews* **442**, 213993.

Sheng, A., Li, X., Arai, Y., Ding, Y., Rosso, K. M. & Liu, J. 2020 Citrate controls Fe(II)-catalyzed transformation of ferrihydrite by complexation of the labile Fe(III) intermediate. *Environmental Science & Technology* **54** (12), 7309–7319.

Shi, X., Ng, K. K., Li, X. R. & Ng, H. Y. 2015 Investigation of intertidal wetland sediment as a novel inoculation source for anaerobic saline wastewater treatment. *Environmental Science & Technology* **49**, 6231–6239.

Sivaranjanee, R. & Kumar, S. P. 2021 A review on remedial measures for effective separation of emerging contaminants from wastewater. *Environmental Technology & Innovation* **23**, 101741.

Sreeja, P. H. & Sosamony, K. J. 2016 A comparative study of homogeneous and heterogeneous photo-Fenton process for textile wastewater treatment. *Procedia Technology* **24**, 217–223.

Thomas, N., Dionysiou, D. D. & Pillai, S. C. 2021 Heterogeneous Fenton catalysts: a review of recent advances. *Journal of Hazardous Materials* **404** (B), 124082.

Tufail, A., Price, W. E., Mohseni, M., Pramanik, B. K. & Hai, F. I. 2021 A critical review of advanced oxidation processes for emerging trace organic contaminant degradation: mechanisms, factors, degradation products, and effluent toxicity. *Journal of Water Process Engineering* **40**, 101778.

Valdés, H., Saavedra, A., Flores, M., Vera-Puerto, I., Aviña, H. & Belmonte, M. 2021 Reverse osmosis concentrate: physicochemical characteristics, environmental impact, and technologies. *Membranes (Basel)* **11** (10), 753.

Vandana, S., Basu, D. B. & Chakravorty, A. K. 2001 Lipid peroxidation, free radical scavenging enzymes, and glutathione redox system in blood of rats exposed to propoxur. *Pesticide Biochemistry and Physiology* **71** (3), 133–139.

Wang, N., Zheng, T., Zhang, G. & Wang, P. 2016 A review on Fenton-like processes for organic wastewater treatment. *Journal of Environmental Chemical Engineering* **4**, 762–787.

Wang, H., Wang, Y. & Dionysiou, D. D. 2023 Advanced oxidation processes for removal of emerging contaminants in water. *Water* **15**, 398.

Wei, Z. & Semiat, R. 2017 Applying a modified Donnan model to describe the surface complexation of chromate to iron oxyhydroxide agglomerates with heteromorphous pores. *Journal of Colloid and Interface Science* **506**, 66–75.

Wei, Z., Luo, S., Xiao, R., Khalfin, R. & Semiat, R. 2017 Characterization and quantification of chromate adsorption by layered porous iron oxyhydroxide: an experimental and theoretical study. *Journal of Hazardous Materials* **338**, 472–481.

Woo, H., Yang, H. S., Timmes, T. C., Han, C., Nam, J. Y., Byun, S., Kim, S., Ryu, H. & Kim, H. C. 2019 Treatment of reverse osmosis concentrate using an algal-based MBR combined with ozone pretreatment. *Water Research* **159**, 164–175.

Xavier, S., Gandhimathi, R., Nidheesh, P. V. & Ramesh, S. T. 2013 Comparison of homogeneous and heterogeneous Fenton processes for the removal of reactive dye Magenta MB from aqueous solution. *Desalination and Water Treatment* **53** (1), 109–118.

Xiang, Q., Nomura, Y., Fukahori, S., Mizuno, T., Tanaka, H. & Fujiwara, T. 2019 Innovative treatment of organic contaminants in reverse osmosis concentrate from water reuse: a mini review. *Current Pollution Reports* **5**, 294–307.

Yaqub, M., Nguyen, M. N. & Lee, W. 2022 Treating reverse osmosis concentrate to address scaling and fouling problems in zero-liquid discharge systems: a scientometric review of global trends. *Science of The Total Environment* **844**, 157081.

Yuan, Y., Garg, S., Wang, Y., Li, W., Chen, G., Gao, M., Zhong, J., Wang, J. & Waite, D. T. 2022 Influence of salinity on the heterogeneous catalytic ozonation process: implications to treatment of high salinity wastewater. *Journal of Hazardous Materials* **423** (B), 127255.

Zhang, H., Gao, H., Cai, C., Zhang, C. & Chen, L. 2013 Decolorization of crystal violet by ultrasound/heterogeneous Fenton process. *Water Science & Technology* **68**, 2515–2520.

Zhang, M.-h., Dong, H., Zhao, L., Wang, D.-x. & Meng, D. 2019 A review on Fenton process for organic wastewater treatment based on optimization perspective. *Science of The Total Environment* **670**, 110–121.

First received 19 March 2023; accepted in revised form 10 May 2023. Available online 19 May 2023